Privileged Communication for
EMBO J

Supplemental Information

CaMKII Binding to GluN2B is Critical During Contextual Memory Consolidation

Amy R. Halt[1#], Robert F. Dallapiazza[1#], Yu Zhou[3,5], Ivar S. Stein[1,2], Hai Qian[1], Scott Juntti[1,4], Sonja Wojcik[4], Nils Brose[4], Alcino J. Silva[3], and J.W. Hell[1,2*]

Departments of [1]Pharmacology
Roy J. and Lucille A. Carver College of Medicine
University of Iowa
Iowa City, IA 52242, USA

[2]Department of Pharmacology, School of Medicine
University of California at Davis
Davis, CA 95616, USA

[3]Department of Neurobiology, Semel Institute, Department of Psychology, Brain Research Institute,
University of California at Los Angeles
Los Angeles, California, 90095, USA.

[4]Department of Molecular Neurobiology
Max Planck Institute of Experimental Medicine
D-37075 Göttingen, Germany

[5]Present Address: Department of Physiology
Medical College of Qingdao University
Qingdao, 266071, China

[#] These two authors contributed equally to this publication

* To whom correspondence should be addressed:
jwhell@ucdavis.edu

Supplemental Figures 1-5
Supplemental Material and Methods
Supplemental References

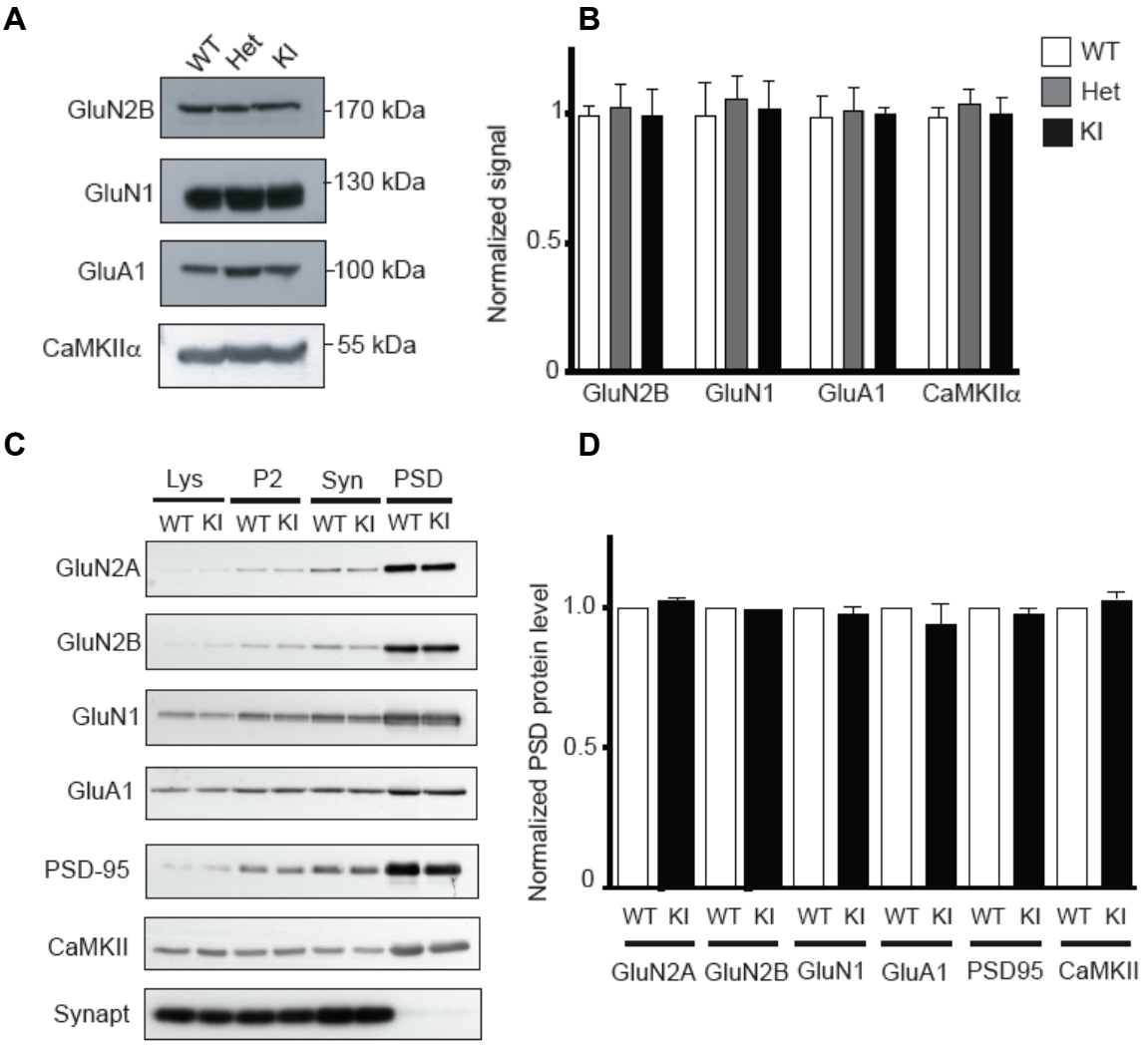

Supplemental Figure 1. Normal protein levels for GluN1, GluN2A, GluN2B, GluA1, PSD-95, CaMKIIα, and synaptophysin in GluN2B KI mice.

(A) Membrane fractions from forebrains of WT and heterozygote (Het) and homozygote GluN2B KI (KI) mice were extracted with 1% deoxycholate before removal of insoluble material by ultracentrifugation. Aliquots containing 30 μg protein were analyzed by IB using antibodies specific for the indicated NMDAR and AMPAR subunits and CaMKIIα. M_R is denoted on the right.

(B) Immunosignals were quantified and Het and KI signals normalized to the WT signal for each repetition. Signals for WT mice were normalized to the average WT signal for all experiments. The data shown represent the average normalized signal intensities +/- SEM for 3 experiments. No statistical significance between WT, Het, and KI mice was seen (p>0.05, one-way ANOVA).

(C) Forebrain lysate from WT (W) and GluN2B KI mice (K) were fractionated by differential centrifugation, sucrose gradient centrifugation and Triton X-100 extraction as described (Lu et al., 2007). 10 μg total protein of the crude lysate (Lys), P2, synaptosomal-enriched (Syn), and PSD fractions were separated via SDS-PAGE and analyzed by IB with antibodies for the indicated proteins including the presynaptic marker synaptophysin (Synapt). Note that GluA1 enrichment is modest compared to NMDAR and PSD-95 (and TARPs; see, e.g., main text Figure 6F) because AMPAR are to a substantial degree extracted from the PSD by Triton X-100, which is required to remove presynaptic elements. The difference in the enrichment of AMPARs vs. PSD-95 and TARPs in PSD preparations indicates that Triton X-100 dissociates to a substantial degree PSD-95 and TARPs from AMPAR during the PSD preparation.

(D) PSD signals were quantified and normalized to the WT signal for each experiment. Illustrated are averages +/- SEM for 3 experiments. Statistical analysis showed no difference for any of the proteins (p>0.05, t-test).

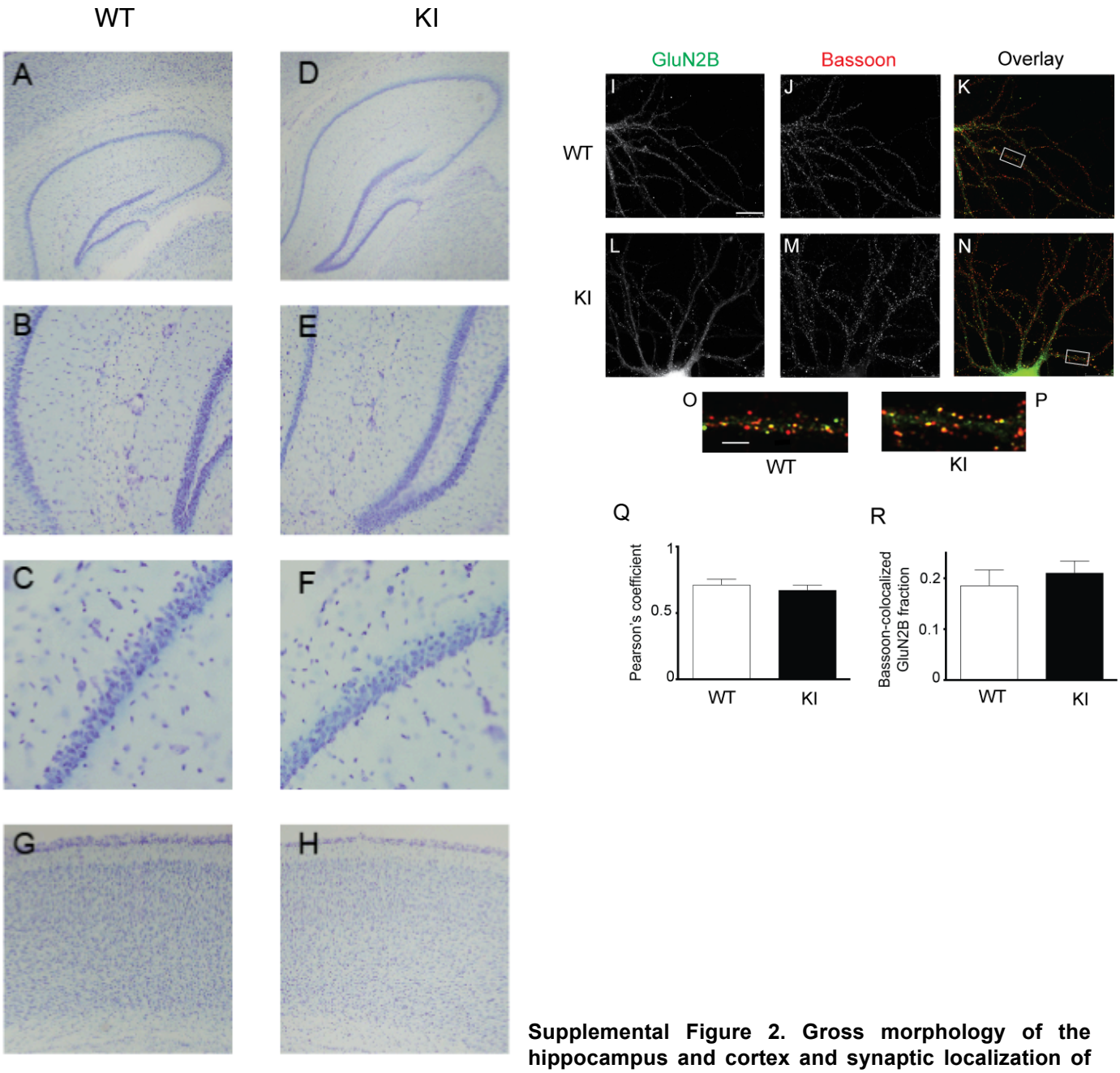

Supplemental Figure 2. Gross morphology of the hippocampus and cortex and synaptic localization of GluN2B are normal in GluN2B KI mice.

(A-H) Nissl stained sections (60 μm) of the hippocampus of WT (A-C) and GluN2B KI mice (D-F) and of cortical layers I-VI from WT (G) and KI (H) mice are comparable (magnification: A,D,G,H: 4x; B,E: 10x; C,F: 40x).

(I-R) Cultured hippocampal neurons from WT and KI mice were immunofluorescently labeled for GluN2B (I, L) and the presynaptic marker Bassoon (J, M) at 20DIV. 25 μm dendritic segments from the overlay images (K, N) were enlarged (O, P) to show the colocalization (yellow) between GluN2B and Bassoon at synapses (scale bars: I: 25 μm; O 5 μm). Images were analyzed using the Image J plug-in JACoP. Colocalization between GluN2B and bassoon was determined using two correlation coefficients based upon the overlap between the red (bassoon) and green (GluN2B) channels: (I) Pearson's coefficient (weighted fraction of pixels that are positive for bassoon and GluN2B), and (J) Mander's coefficient (the fraction of GluN2B positive pixels independent of intensity that were colocalized with bassoon positive pixels; all analysis was performed after thresholding). The data represent the average +/- SEM for 10 neurons per condition per experiment from 3 experiments. No statistical difference was found between WT and KI neurons for either correlation coefficient (p>0.05, Student's t-test).

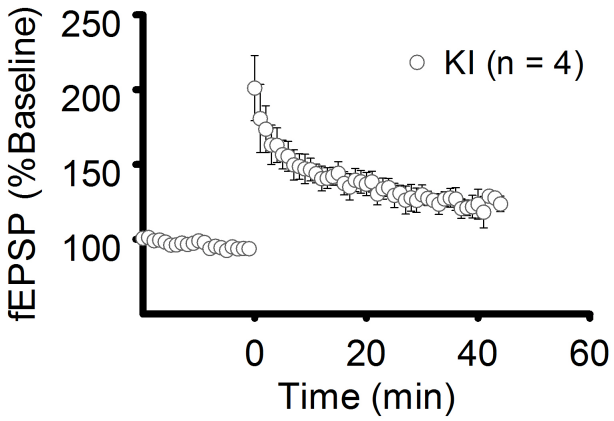

Supplemental Figure 3. Two-tetanus LTP in WT and GluN2B KI Mice is not Inhibited by H-89.
LTP was induced at time point 0 by 2 tetani of 100Hz/1s, 10 s apart, in CA1 in acute hippocampal slices in the presence of H-89 (20 μM). It stabilized at 130.2±5.5% of baseline (mean±SEM) in KI slices (above), which is comparable to and in fact slightly above the level of the reduced LTP in KI mice in the absence of any drugs (see main text Figure 4A). As we found earlier (Lu et al., 2007), H89 did also not affect LTP induced by 2 tetani of 100 Hz in WT slices, which stabilized at 150.9±6.9% of baseline comparable to 100 Hz LTP in WT slices (see main text Figure 4A).

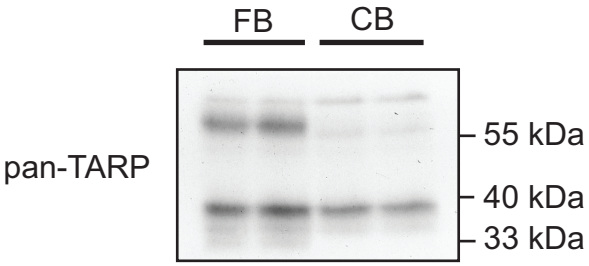

Supplemental Figure 4. Pan-TARP antibody specificity.
Crude membrane extracts from forebrain (FB) and cerebellum (CB) were used for characterization of a pan-TARP antibody by IB. This antibody had been raised against a peptide with a sequence common to all four of the closely related conventional TARPs (stg/γ2, γ3, γ4, γ8) but not the more distantly related γ1, γ5, γ6, or γ7 (Letts et al., 1998). As expected (e.g., (Nakagawa et al., 2005)), in FB the antibody recognized three bands in the 30-40 kDa range that match the molecular weights of γ2, γ3, and γ4, which are similar, and a prominent band around 55 kDa corresponding to the larger γ8 (see also Figure 6F). In cerebellar extracts, the immunoreactivity is reduced for the lower two bands suggesting that those bands represent γ3 and γ4 and near absent for the upper band indicating that this band corresponds to γ8 as γ3 and γ4 are only weakly expressed and γ8 is near absent in the cerebellum (Chen et al., 2000; Menuz and Nicoll, 2008; Menuz et al., 2008; Tomita et al., 2003). The remaining, strong band just below the 40 kDa marker is thus most likely stg/γ2. The figure is representative of 3 experiments.

Supplemental Experimental Procedures

Mice

All animal procedures were approved by the University of Iowa, UC Davis and UCLA Animal Care and Use Committees and followed NIH guidelines. Heterozygous GluN2B KI mice (Supplemental Figure 4) were bred to obtain homozygous GluN2B KI mice and litter-matched WT controls. All experiments (biochemical, cell biological, electrophysiological, and behavioral) were conducted with litter-matched WT and GluN2B KI mice.

In the targeting vector for the GluN2B KI mice, a Neomycin resistance gene flanked by two loxP sites was inserted in sense orientation 140 bp 3' of the stop codon of the GluN2B gene between a 2.3 kb 5' short arm (containing the large last coding exon with the stop codon, i.e. exon 13, 305 bp of 5' flanking intronic sequence, and 140 bp of 3' untranslated exonic sequence) and a 3' 3.1 kb BamHI/SpeI genomic fragment as long arm (starting 140 bp 3' of the stop codon and containing the entire remaining part of the 3' untranslated exonic sequence and 890 bp of the 3' intronic sequence) (Supplementary Fig. 1A). Two copies of the HSV thymidine kinase gene were attached 5' to the short arm for negative selection of randomly integrated vector. The short arm was generated by PCR using SV129J mouse genomic DNA as template. Three point mutations were introduced to generate the L1298A and R1300Q mutations and a BssHII site for diagnostic purposes. The targeting construct was linearized by digestion with NotI and electroporated into the E14 ES cell line. Homologously recombined cells were selected in the presence of G418 (positive selection) and Ganciclovir (negative selection against random integration). Homologous recombination was verified by diagnostic PCR with a 5' primer (5'-CCCGGCGTTCTTCATCAATACTAA-3') 500 bp upstream of the 5' end of the short arm and a 3' primer (5'-CTCACCAGCTGGCATCTCAAACAT) 143 bp 3' of the diagnostic BssHII site and the L1298A and R1300Q mutations and subsequent digestion with BssHII. This PCR results in the amplification of 2.24 kb fragments from WT and KI loci and allows to distinguish WT and KI amplicons by digestion with BssHII, which yields a 2.10 kb fragment for the knock-in allele only (cf. Supplementary Fig. 1B). Positive clones were injected into C57BL/6J blastocysts, which were transferred to female mice. Founder chimeras were backcrossed 7 generations with C57BL/6J mice (all C57BL/6J mice were obtained from Taconic) and with EIIa/Cre mice to excise the Neo cassette. Over time additional back crossings were performed with C57BL/6J mice to avoid issues due to extensive inbreeding. Subsequent routine genotyping was performed by non-diagnostic PCR, using primers flanking the mutation site (5' oligonucleotide: 5'-CATCTCCACGCATACTGTCAC-3'; 3' oligonucelotide: 5'-CTCACCAGCTGGCATCTCAAACAT-3') and subsequent digestion with BssHII).

Preparation and Treatment of Acute Forebrain Slices

Transverse slices (350 μM thick) were prepared at 24°C with a Leica VT1000S vibrating microtome in (in mM) 127 NaCl, 26 $NaHCO_3$, 1.2 KH_2PO_4, 1.9 KCl, 1 $CaCl_2$, 2 $MgSO_4$, 10 dextrose (saturated with 95% O_2 and 5% CO_2) and transferred after 60 min to 32°C oxygenated artificial cerebrospinal fluid (ACSF; in mM: 127 NaCl, 26 $NaHCO_3$, 1.2 KH_2PO_4, 1.9 KCl, 2.2 $CaCl_2$, 1 $MgSO_4$, 10 dextrose). To specifically stimulate Ca^{2+} influx through NMDAR and prevent general neuronal excitation, slices were pre-treated with 1 μM TTX for 5 min before addition of 200 μM NMDA vs. vehicle (H_2O) for 5 min (Leonard et al., 1999). To chemically induce LTP (cLTP) slices were treated with 50 μM forskolin vs. vehicle (0.01% DMSO) for 15 min before transfer to ACSF containing 30 mM K^+ and 0 mM Mg^{2+} vs. normal ACSF, respectively, (see (Lu et al., 2007)). After 5 min slices were extracted either immediately or after 30 min in normal ACSF.

Isolation of PSDs

3-4 forebrains (or 2 forebrain slices) were homogenized in 15 mL (0.5 ml) 0.32 M sucrose, 1 mM $MgCl_2$, 1 mM HEPES, pH 7.0, plus protease inhibitors (Leonard et al., 1998) and centrifuged at low speed (2,500 rpm, 10 min) and high speed (20,000 rpm, 20 min; P2). P2 was resuspended in 0.32 M sucrose/1 mM HEPES for sucrose step gradient centrifugation (0.85/1/1.25 M; 24,000 rpm, 2 h) (Lu et al., 2007). The synaptosome fraction (Syn) at the 1/1.25 M interface was treated with 0.5% Triton X-100 and centrifuged (24,000 rpm, 30 min). The pellet (Tx-1) was resuspended in 0.32 M sucrose/1 mM HEPES for sucrose step gradient centrifugation (1/1.5/2.0 M; 35,000 rpm, 2 h) to obtain the PSD

fraction at the 1.5/2.0 interface (Lu et al., 2007). Protein concentrations were determined with bicinchoninic acid. For preparation of a crude fraction enriched for PSD from acute slices, the P2 fraction was treated with Tx-100, as above, to isolate the PSD-containing fraction by subsequent ultracentrifugation (pellet).

Immunoprecipitation and Immunoblotting
A crude forebrain membrane fraction or slices were extracted with 1% deoxycholate and non-solulbe material removed by ultracentrifugation before immunoprecipitation and quantitiative IB (see e.g., (Merrill et al., 2007)) with antibodies against CaMKIIα, CaMKIIβ, CaMKIIα - phospho-T286, GluN1, GluN2A, GluN2B, GluA1, GluA1 - phospho-S831, PSD-95, and synaptophysin as described earlier (Leonard et al., 1998; Leonard et al., 1999; Lu et al., 2007). The pan-TARP antibody was kindly provided by Dr. K. P. Campbell (University of Iowa, Iowa City, IA).

Primary Hippocampal Cultures and Immunofluorescence Microscopy
Cultures were prepared from individual litter-matched WT and KI P0 pups as described using Neurobasal medium (Invitrogen) supplemented with NS21 (Chen et al., 2008). Following stimulation with glutamate or vehicle, neurons were briefly washed with PBS (phosphate buffered saline: 137 mM NaCl, 3 mM KCl, 10 mM NaH_2PO_4, 1 mM KH_2PO_4, pH 7.4) and fixed in 4% paraformaledehyde (PFA)/4% sucrose/PBS for 15 min at room temperature for CaMKII/synapsin labeling or thoroughly dehydrated methanol at -20°C for 10 min for GluN2B/bassoon labeling. Coverslips were washed with PBS 3x5 min. Neurons were permeabilized with 0.5% Triton X-100/PBS for 20 min. Coverslips were washed again (PBS, 2x5 min) and blocking solution (5% FBS, 2% goat serum, 2% glycerol, 50 mM NH_4Cl, PBS) was applied for 2h at RT. Primary antibodies were diluted in blocking solution for incubation of coverslips overnight at 4°C. The following antibody dilutions were used: CaMKIIα 1:500, synapsin 1:1000, GluN2B 1:200, bassoon 1:1000. The monoclonal mouse antibody against CaMKIIα and rabbit antibody against GluN2B were as above, the rabbit antibody against synapsin from Dr. P. DeCamilli (Yale University, New Haven, CT) (Bartos et al., 2010) and the monoclonal mouse antibody against bassoon from Stressgen (VAM-PS003). Neurons were washed 3x5min with PBS, and blocking solution was applied for 30 min at RT. Alexa-conjugated secondary antibodies (Bartos et al., 2010) were diluted in blocking solution and incubated with coverslips for 1h at RT. The coverslips were washed with PBS, 4x5min, then water, 3x5min. The coverslips were mounted on glass slides using Prolong Antifade Gold Reagent (Molecular Probes). Coverslips were allowed to dry for 24h at RT before storing at -20°C prior to imaging.

Images were taken using a Leica epifluorescence microscope with a 63X objective. The images were collected blinded, with identical exposure, gain, and intensity settings for each fluorophore. Correlation coefficients were determined blind, using an ImageJ (National Institutes of Health) plugin, JACoP. Images were thresholded equally prior to analysis.

Recording and analysis of field excitatory postsynaptic potentials (fEPSPs), LTP, and LTD
Forebrain slices were trimmed and perfused with oxygenated ACSF (in mM: 127 NaCl, 26 $NaHCO_3$, 1.2 KH_2PO_4, 1.9 KCl, 2.2 $CaCl_2$, 1 $MgSO_4$, 10 glucose) in a submersion chamber at a rate of 2 ml/min at 32°C. (Lu et al., 2007). After 10 min equilibration, an ACSF filled glass electrode was positioned in the stratum radiatum of the CA1 region of the hippocampus, and a bipolar tungsten electrode (World Precision Instruments) was adjacently positioned. Field EPSPs were evoked by 0.1 msec stimulation of the Schaffer collaterals at 0.067 Hz. Field potentials were amplified with an AxoClamp 2B amplifier, filtered at 1 kHz, digitized at 10 kHz with Axon Digidata 1200 (Axon Instruments), and stored on a PC hard drive. Field EPSP rising slopes were calculated using Clampfit 9 software (Axon Instruments). The average slope of the baseline recordings were used to normalize the response. Field potentials with absolute amplitudes <0.5 mV or unstable fiber volley amplitudes were discarded. Stimulation intensity was adjusted to evoke a synaptic response that was 40-60% of the maximum. Baseline responses were recorded for 10-15 minutes prior to conditioning stimuli. LTP or LTD were induced using one of the following stimulation protocols: 10 Hz for 15 sec, 100 Hz for 1 sec, theta burst stimulation (10 stimulus trains at 5 Hz, each consisting of 5 stimuli at 100 Hz), or 1 Hz for 900 sec.

Recording and analysis of mini-excitatory postsynaptic currents (mEPSCs)
Pyramidal neurons in the CA1 of acute hippocampal slices were visualized under infrared with a BX50WI inverted microscope. Neurons were patch-clamped in the whole-cell configuration with a borosilicate glass electrode (2-4 MΩ) filled with (in mM): 125 K-Gluconate, 10 KCl, 3 Mg-ATP, 1 $MgCl_2$, 10 HEPES, pH 7.25, 290 mOsm. Holding potentials (V_{hold}) were –70 mV. Slices were superfused with ACSF. AMPAR-mediated mEPSC were recorded in the presence of 200 nM TTX to block action potentials, 10 μM bicuculline to block GABAA receptors, and 50 μM AP5 to block NMDAR. Criteria for data inclusion in the analysis were: (1) stable series resistance <25MΩ; (2) stable input resistance >100MΩ. Series resistance was monitored by a 50 msec depolarizing pulse from –60 to –55 mV before and after recording. AMPAR mediated mEPSC frequency, amplitude, and decay constant were calculated (pClamp 9, Axon Instruments) and expressed as mean values using SEM for variance.

Open field analysis
General behavior and locomotor activity was evaluated in the open-field test. Mice were individually placed in a square open field made of acrylic (27 x 27 x 20.3 cm) in a dimly lit room. Activity was recorded by an automated system (Med Associates) for 20 min via 16 photobeams spaced evenly apart on both *x*- and *y*-axes. The chambers were washed thoroughly with Windex between individual experiments. Ambulatory distance (average of distances traveled within 1 min during a 20 min period), jump counts and vertical activity counts over a 20 min period were the primary measures for exploratory activity. Zone analysis was performed to determine outer sector occupancy of mice; high scores in this measure can indicate high anxiety levels.

Trimethyl-thiazoline (TMT) response
Mice were placed in a 10x10x10 cm Plexiglas chamber containing a beaker with TMT (30 μl, 1M), an active component of fox urine. Mice were video recorded and subsequently scored for time spent freezing. Freezing was defined as an absence of movement except motion that was necessary for respiration and was measured by a trained observer who was blinded to the genotype of the mice.

Accelerating RotaRod test
The mice observed in the open field were subsequently tested on the RotaRod. The RotaRod consisted of a drum (outer diameter: 1¼ inch) made of ribbed plastic and panels that separated the apparatus into five lanes (Technical and Scientific Equipment). Mice were placed on the RotaRod while it was rotating at 5 rpm. As soon as all mice were placed on the apparatus, the acceleration and timer were activated and rotational speed steadily increased from 5 to 60 rpm over the course of 3 min. Trials were terminated after 3 min or when the mice fell off the rod. The time elapsing from the beginning of acceleration to fall down of a mouse was automatically recorded. On each day, every mouse was tested three times sequentially with 2h inter-trial intervals. The average of the latencies of the three trials on a give day was calculated.

Morris water maze tasks
The same mice used in the RotaRod test were analyzed in the MWM after a one month break. Another cohort was tested without any other previous testing. Mice were extensively handled (3 min every day for 7 days) before starting the MWM training and tests. On the first day of training, the mice are placed on the platform for 30 s in a round pool (diameter: 1.2 m) filled with opaque water. They were allowed one 30 s practice swim as well as three platform climbs. They were permitted to rest for another 30 s on the platform. Then the first training trial was initiated. Mice were placed facing the pool wall away from the platform. The starting position was varied from trial to trial. The platform location is fixed for the training period. The mice were allowed to swim until they found the submerged escape platform or maximally 60 sec (for further details see (Bourtchuladze et al., 1994)). Mice were given two blocks (1h inter-block interval; IBI) of two trials (30 s inter-trial interval; ITI) every day for 6 days. Spatial learning and memory was assessed in 60 sec probe tests after removal of the platform 1h after the end of training on day 3 and 5 and either 1 or 3 days after the end of the last training on day 6. The search pattern of the mice was recorded by a CCD camera and analyzed by using VHS software. For the visible platform task, the platform was marked with a visible cue (colored

ball). Mice were given two blocks (1h IBI) of four trials (30 s ITI) per day, using a fixed platform position and with changes of the starting position in each new trial, with now significant difference between genotypes.

Delayed spatial win-shift eight-arm radial-maze task

Mice were habituated to the maze during the first two days. Subsequent daily training session consisted of two distinct phases (A and B), separated by a 2 min delay. In phase A, food-deprived animals were allowed to enter four of the eight maze arms (Bioserv, Frenchtown, NJ) and obtain a reward pellet from each arm. In phase B, all eight arms were open. Only the four arms that were not open in phase A contained a reward in phase B. For correct performance, mice had to remember the location of food in phase A and enter the new arms in phase B. Performance was gauged by the ratio [number of correct arm entered]/[total number of arms entered] during phase B. Mice had a maximum of 5 min to retrieve the four pellets during phase A and B. To be recorded as an arm entry a mouse had to run down the entire length of an arm and reach the food cup at the end. The latencies for reaching the food cup of the first arm visited and for completing the phase were also recorded.

Mice were trained for 10 consecutive days with this arrangement. Subsequent tests evaluated the performance with increased interphase intervals between phase A and B.

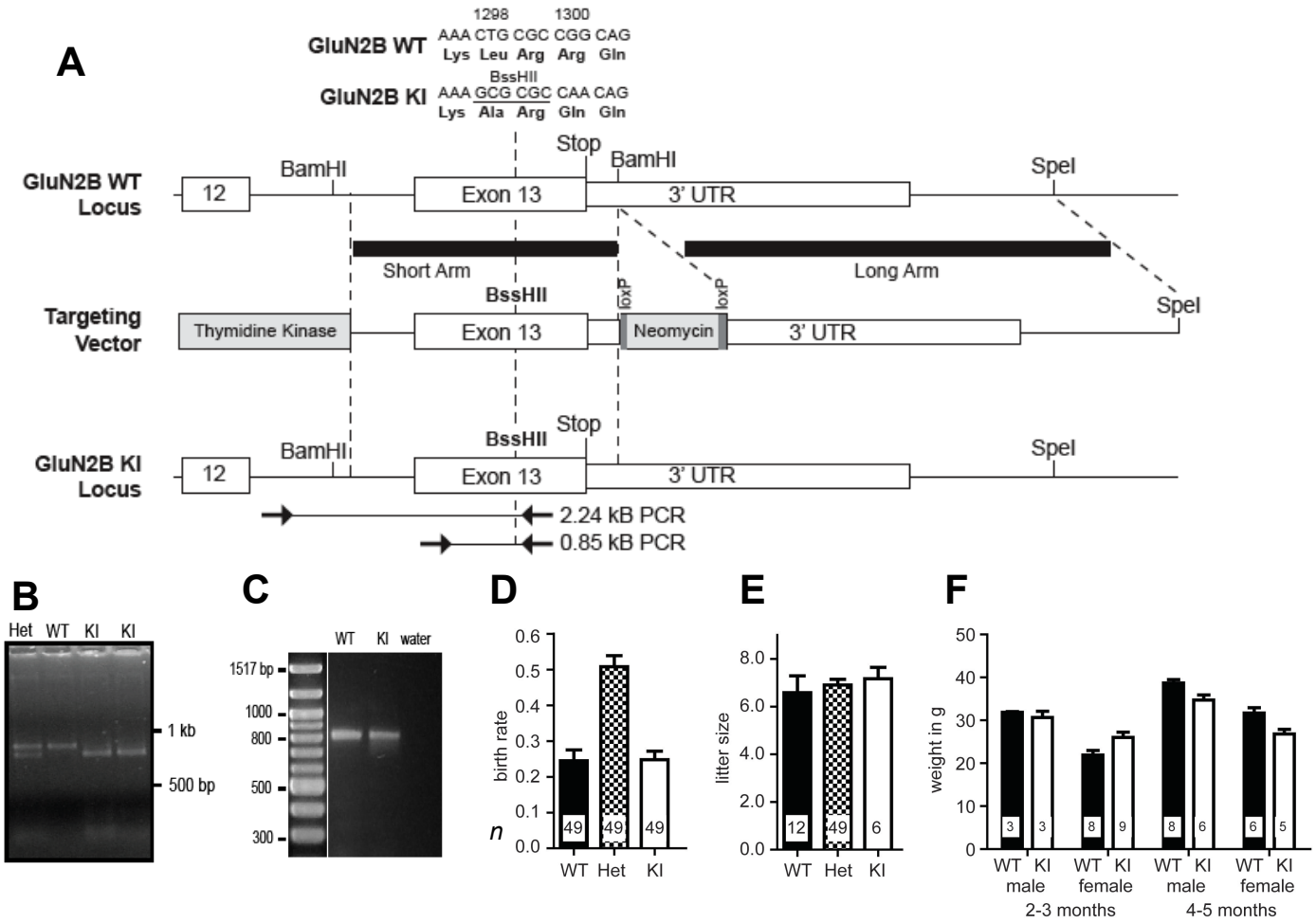

Supplemental Figure 5. Creation and Genotyping of GluN2B KI Mice.

(**A**) Targeting vector and homologous recombination. A Neomycin resistance gene flanked by two loxP sites was inserted downstream of the last exon (exon 13) of the GluN2B gene. Two copies of the HSV thymidine kinase gene were inserted in the intron preceding exon 13. Three point mutations created L1298A and R1300Q mutant GluN2B and a BssHII site for diagnostic purposes. E14 ES cell were electroporated with linearized vector. Homologously recombined cells were treated with G418 (positive selection) and Ganciclovir (negative selection), confirmed by diagnostic PCR (similar to **B**), and injected for germline transmission.

(**B**) Routine PCR genotyping identified homozygous WT mice by a single 853 bp undigested fragment, homozygous KI mice by 2 bands with 709 and 144 bp due to the complete digestion of the amplicon by BssHII, and heterozygous (het) mice by the presence of all 3 bands.

(**C**) Homologous recombination was verified in GluN2B KI mice by diagnostic PCR of mouse tail DNA with a 5' primer 800 bp upstream of exon 13 and a 3' primer overlapping the beginning of exon 13. The generation of the 800 bp PCR fragment and successful diagnostic BssHII digestion from panel (B) indicates that integration of the targeting vector occurred at the GluN2B locus.

(**D**) Normal birth rate of heterozygous and homozygous GluN2B KI mice from heterozygous breeders as monitored between June 2010 and April 2011 after 10 back crossings with C57BL/6J from Taconic Farms.

(**E**) Normal offspring size from homozygous and heterozygous GluN2B KI vs C57black/6 WT breeders as monitored between June 2010 and April 2011.

(**F**) Normal weight of homozygous GluN2B KI mice vs litter mate WT mice for different sexes and ages as monitored between June 2010 and April 2011.

Supplemental References

Bartos, J.A., Ulrich, J.D., Li, H., Beazely, M.A., Chen, Y., Macdonald, J.F., and Hell, J.W. (2010). Postsynaptic clustering and activation of Pyk2 by PSD-95. J Neurosci *30*, 449-463.

Bourtchuladze, R., Frenguelli, B., Blendy, J., Cioffi, D., Schutz, G., and Silva, A.J. (1994). Deficient long-term memory in mice with a targeted mutation of the cAMP-responsive element-binding protein. Cell *79*, 59-68.

Chen, L., Chetkovich, D.M., Petralia, R.S., Sweeney, N.T., Kawasaki, Y., Wenthold, R.J., Bredt, D.S., and Nicoll, R.A. (2000). Stargazing regulates synaptic targeting of AMPA receptors by two distinct mechanisms. Nature *408*, 936-943.

Chen, Y., Stevens, B., Chang, J., Milbrandt, J., Barres, B.A., and Hell, J.W. (2008). NS21: re-defined and modified supplement B27 for neuronal cultures. J Neurosci Methods *171*, 239-247.

Leonard, A.S., Davare, M.A., Horne, M.C., Garner, C.C., and Hell, J.W. (1998). SAP97 is associated with the a-amino-3-hydroxy-5-methylisoxazole-4-propionic acid receptor GluR1 subunit. J Biol Chem *273*, 19518-19524.

Leonard, A.S., Lim, I.A., Hemsworth, D.E., Horne, M.C., and Hell, J.W. (1999). Calcium/calmodulin-dependent protein kinase II is associated with the N-methyl-D-aspartate receptor. Proc Natl Acad Sci USA *96*, 3239-3244.

Letts, V.A., Felix, R., Biddlecome, G.H., Arikkath, J., Mahaffey, C.L., Valenzuela, A., Bartlett, F.S., 2nd, Mori, Y., Campbell, K.P., and Frankel, W.N. (1998). The mouse stargazer gene encodes a neuronal Ca2+-channel gamma subunit. Nature Genetics *19*, 340-347.

Lu, Y., Allen, M., Halt, A.R., Weisenhaus, M., Dallapiazza, R.F., Hall, D.D., Usachev, Y.M., McKnight, G.S., and Hell, J.W. (2007). Age-dependent requirement of AKAP150-anchored PKA and GluR2-lacking AMPA receptors in LTP. EMBO J *26*, 4879-4890.

Menuz, K., and Nicoll, R.A. (2008). Loss of inhibitory neuron AMPA receptors contributes to ataxia and epilepsy in stargazer mice. J Neurosci *28*, 10599-10603.

Menuz, K., O'Brien, J.L., Karmizadegan, S., Bredt, D.S., and Nicoll, R.A. (2008). TARP redundancy is critical for maintaining AMPA receptor function. J Neurosci *28*, 8740-8746.

Merrill, M.A., Malik, Z., Akyol, Z., Bartos, J.A., Leonard, A.S., Hudmon, A., Shea, M.A., and Hell, J.W. (2007). Displacement of alpha-Actinin from the NMDA Receptor NR1 C0 Domain By Ca(2+)/Calmodulin Promotes CaMKII Binding. Biochemistry *46*, 8485-8497.

Nakagawa, T., Cheng, Y., Ramm, E., Sheng, M., and Walz, T. (2005). Structure and different conformational states of native AMPA receptor complexes. Nature *433*, 545-549.

Tomita, S., Chen, L., Kawasaki, Y., Petralia, R.S., Wenthold, R.J., Nicoll, R.A., and Bredt, D.S. (2003). Functional studies and distribution define a family of transmembrane AMPA receptor regulatory proteins. J Cell Biol *161*, 805-816.